

Self-Association Patterns of Sodium Taurocholate and Taurodeoxycholate As Studied by Frontal Derivative Chromatography

Noriaki Funasaki,* Sakae Hada, and Saburo Neya

Kyoto Pharmaceutical University, Misasagi, Yamashina-ku, Kyoto 607-8414, Japan

Received: July 28, 1998; In Final Form: November 9, 1998

The aggregation patterns of sodium taurocholate (TC) and taurodeoxycholate (TDC) in an isotonic sodium chloride solution at 298.2 K are investigated by frontal derivative chromatography on Sephadex G-10 columns and are quantitatively analyzed on the basis of several aggregation models. The aggregation parameters are best fitted to the observed centroid volume data. The derivative chromatogram of TC at 6.006 mM simulated on the basis of a stepwise aggregation model is in excellent agreement with the observed one, whereas the simulation on the basis of the pentamerization model remarkably differs in shape from the observed one. The derivative chromatograms of TDC at 1.500 and 2.003 mM simulated on the basis of another stepwise aggregation model are closer to the observed ones than those of the Bottari–Festa model. Thus, TC and TDC form their dimers and polydisperse micelles. These conclusions are supported by the fitness to the centroid volume data. In light of the present results and current reports, the structure and counterion binding of bile salt micelles are discussed.

Introduction

The micellization of bile salts plays a critical role in the digestion of lipids in animals. Many studies on this topic have been reported and reviewed in monographs^{1,2} and a review article.³

In 1994, we reported aggregation numbers, critical micellization concentrations, stepwise aggregation constants, and aggregation models for sodium taurocholate (TC) and taurodeoxycholate (TDC) in a 154 mM sodium chloride solution at 298.2 K.⁴ We determined the dimerization constants of TC and TDC on the basis of gel filtration chromatographic (GFC) data, such as the centroid volume and the position and height of the trailing peak.⁴ The validity of these methods has been demonstrated for chlorpromazine hydrochloride and methylene blue by comparison with UV spectrophotometry.^{5–7} Recently, several models for the micellization of bile salts have been proposed for bile salts.^{8–12} The presence^{4,8,9} or absence^{10–12} of dimer and monodispersity^{10,11} or polydispersity^{4,8,9,13} in micelle size are matters of controversy among these models.

In the present work we provide further chromatographic evidence for our stepwise aggregation models for TC and TDC. The frontal derivative chromatogram of the dimerizing system has a single peak, which shifts to the smaller elution side with increasing concentration. On the other hand, those of higher polymerizing systems exhibit bimodality.^{5,6,14} This characteristic pattern of dimerization can be used to detect dimer in the presence of other multimers and to resolve the above controversy on the aggregation patterns of TC and TDC.

Experimental Section

Materials. Specimens of TC (Calbio) and TDC (Sigma) were treated with charcoal in methanol three times and recrystallized from methanol. The crystals were freeze-dried from water

several times and dried at 383 K under reduced pressure. The purified samples of TC and TDC were both 99.0% pure or more, as estimated by high-performance liquid chromatography.⁴ Sephadex G-10 (Pharmacia) columns were treated as suggested by the manufacturer. The double-distilled water was degassed just before each GFC experiment.

Methods. All GFC experiments were carried out in a 154 mM sodium chloride solution under a flow rate of ca. 0.4 cm³ min^{−1}. Different columns were used for TC and TDC. The columns were jacketed in order to maintain them at a constant temperature of 298.2 ± 0.2 K. The concentration of a bile salt in eluate was monitored continuously with a differential refractometer and an absorbance detector (at a wavelength of 220 nm). The flow rate was also monitored with an electrobalance. These data were saved in a computer for further analysis. The chromatographic data were subjected to the treatments of smoothing and baseline corrections. The GFC experiments were carried out at a number of concentrations; the numbers *n* of data points are 13 for TC and 19 for TDC. The derivative chromatogram was approximated by the difference chromatogram.

Simulations of chromatograms were carried out by a plate theory (continuous flow model).¹¹ The number of the plate (*N*) and the void volume of the column are the same as those already reported (*N* = 35 for TC and *N* = 25 for TDC).⁴

Further details on experiments and calculations were reported elsewhere.^{4,5}

Results and Discussion

Self-Association of TC. A large volume of a dilute TC solution was applied on the Sephadex G-10 column, so that the plateau region appeared on the chromatogram. This chromatogram is termed the frontal chromatogram. Because the concentration *C* of TC in the plateau is the same as that applied, this chromatogram affords us quantitative information on the self-association of TC. Because the centroid volumes, *V*_c' and *V*_c, at

* Phone: +81-75-595-4663. Fax: +81-75-595-4762. E-mail: funasaki@mb.kyoto-phu.ac.jp.

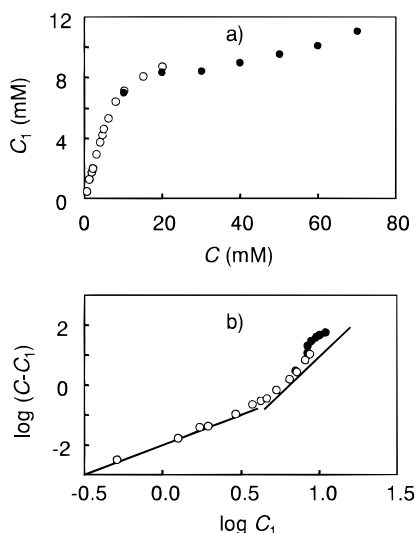


Figure 1. (a) Plots of monomer concentration data against the total concentration of TC and (b) plots of $\log(C - C_1)$ versus $\log C_1$, on the basis of monomer concentration data obtained for TC by Funasaki et al. (open circles)⁴ and Lee et al. (closed circles).¹⁵ The straight lines show slopes of $n_w = 2$ and 5.

the leading and trailing boundaries were equal to each other within experimental errors, we took the average of them as V_c .

As we have shown,⁵⁻⁷ we can determine the monomer or intermicellar concentration C_1 from

$$C_1 = (V_m - V_c)C / (V_1 - V_m) \quad (1)$$

Here V_1 and V_m denote the centroid volumes of the monomer and micelle of TC, respectively: $V_1 = 29.30 \text{ cm}^3$ and $V_m = 9.89 \text{ cm}^3$. The GFC experiments were carried out at 13 different TC concentrations. Figure 1a shows the observed monomer concentration (open circles) as a function of the total TC concentration. The monomer concentration data, determined by the Sephadex G-10 beads uptake method at 303 K by Lee et al.,¹⁵ are also shown by closed circles. Ammon and Walter developed this method to determine the monomer concentrations of TC and TDC at room temperature.¹⁶ The Ammon–Walter data are very close to ours,¹⁶ although they are not included in Figure 1. The Lee et al. data are not distant from ours but seem to be inaccurate at high TC concentrations. This is shown more clearly in Figure 1b.

According to multiple equilibrium theory for self-association,^{6,7,17} the micellar weight average aggregation number n_w is calculable from

$$n_w = d \log(C - C_1) / d \log C_1 \quad (2)$$

Our data show that TC forms dimer at low concentrations and larger multimers at higher concentrations. We reported the aggregation number as a function of the total TC concentration.⁴ On the other hand, the Lee et al. data show that the micellar weight average aggregation number of TC decreases with increasing concentration. This contradicts the thermodynamic prediction.¹⁷ On the basis of the Lee et al. data, Liu proposed that TC forms pentamer alone independent of its total concentration.¹¹

The other piece of evidence against the pentamerization model of TC comes from the derivative chromatogram of TC. We have proposed many aggregation models for the self-association of TC and shown that model II-10 is the best model among them. This is a stepwise aggregation model:

$$A_{i-1} + A_1 \xrightleftharpoons{k_i} A_i \quad (i = 2, 3, 4, \dots, \infty) \quad (3)$$

$$k_i = [A_i] / [A_{i-1}]C_1 \quad (4)$$

The stepwise aggregation constants k_i for model II-10 have already been reported as a function of aggregation numbers i . In model II, we assumed a marked attenuation (anticooperativity) of k_i at large aggregation numbers; that is, $ik_i = (i + 1)k_{i+1} = \dots = k$. The total concentration of TC can be written as

$$C = C_1 + 2k_2C_1^2 + \dots + (i - 1)K_{i-1}C_1^{i-1} + (i - 1)!K_{i-1}C_1^{i-2}[\exp(kC_1) - 1 - kC_1 - (kC_1)^2/2! - \dots - (kC_1)^{i-2}/(i - 2)!] \quad (5)$$

Here $K_i = k_2k_3\dots k_i$, $ik_i = (i + 1)k_{i+1} = \dots = k = 1100 \text{ M}^{-1}$, $k_2 = 6.11 \text{ M}^{-1}$, $k_3 = 1.2 \text{ M}^{-1}$, $k_4 = 420 \text{ M}^{-1}$, $k_5 = 200 \text{ M}^{-1}$, $k_6 = 3180 \text{ M}^{-1}$, $k_7 = 6 \text{ M}^{-1}$, $k_8 = 150 \text{ M}^{-1}$, $k_9 = 130 \text{ M}^{-1}$, and $k_{10} = 150 \text{ M}^{-1}$. These stepwise aggregation constants were determined by minimizing the sum, SS, of the squares of the differences in V_c between theory and experiment:

$$SS = \sum_1^n (V_{c,\text{calcd}} - V_{c,\text{obsd}})^2 \quad (6)$$

Here n stands for the number of data points; $n = 13$ for TC. The SS value is 0.0205 cm^6 .⁴

The pentamerization model is written as

$$5A_1 \xrightleftharpoons{K_5} A_5 \quad (7)$$

$$K_5 = [A_5] / C_1^5 \quad (8)$$

$$C = C_1 + 5K_5C_1^5 \quad (9)$$

Using our observed V_c data, we determined the best fit pentamerization constant of $K_5 = 1.718 \times 10^{-4} \text{ M}^{-4}$ and the SS value of 1.0997 cm^6 . Judging from these SS values, model II-10 is better than the pentamerization model.

The derivative chromatogram at the trailing boundary reflects the aggregation pattern. The derivative chromatogram of the dimerizing system uniquely has a single peak, whereas those of the other multimerizations exhibit bimodality.^{5-7,14} This characteristic feature of dimerization can be used for detecting dimer in the presence of other multimers. Figure 2 shows the derivative chromatogram of TC at $C = 6.006 \text{ mM}$, which is a slightly lower concentration than a cmc of 6.3 mM . It is particularly noted that the observed peak ($V_p = 27.26 \text{ cm}^3$) shifts slightly to the lower elution volume side than the monomer peak at $V_{1p}^0 = 29.26 \text{ cm}^3$. This tendency is characteristic of dimerization. Model II-10 ($V_p = 27.10 \text{ cm}^3$) very well reproduces the observed chromatogram. On the other hand, the chromatogram predicted by the pentamerization model has the peak ($V_p = 28.37 \text{ cm}^3$) due to the monomer and has a shoulder around 22 cm^3 . This shoulder is a symptom of appearance of the second peak.

Thus, model II-10 is superior to the pentamerization model.

Self-Association of TDC. We proposed that model IV-8, a stepwise aggregation model, is the best among many aggregation models for TDC.⁴ According to this model, the total TDC concentration can be written as

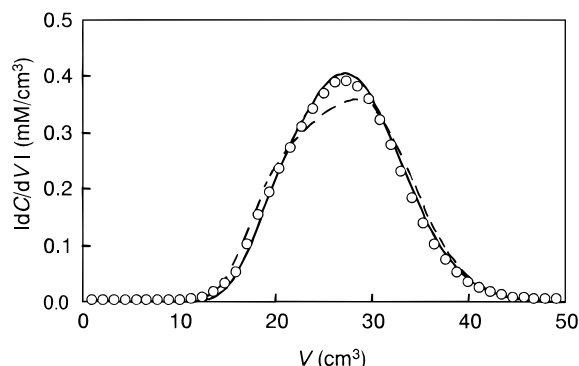


Figure 2. Derivative chromatograms of TC at $C = 6.006$ mM: (○) observed results; (—) simulation on the basis of our IV-10 model; (---) simulation on the basis of the pentamerization model.

$$C = C_1 + 2k_2C_1^2 + \dots + 6k_2k_3k_4k_5k_6C_1^6 + \sum_{i=7}^{\infty} iC_1^i \exp(ai - bt^{2/3} - ct^{4/3}) \quad (10)$$

Here $k_2 = 16.1 \text{ M}^{-1}$, $k_3 = 1.8 \text{ M}^{-1}$, $k_4 = 4700 \text{ M}^{-1}$, $k_5 = 600 \text{ M}^{-1}$, $k_6 = 3200 \text{ M}^{-1}$, $a = 5.47$, $b = 9.26$, and $c = 1.05$. The term a corresponds to the driving force of micellization due to the transfer of the hydrophobic group from water to the micelle. The term b expresses the reduction of hydrophobic surface area caused by spherical micelle formation. The term c denotes the electrostatic repulsion between the hydrophilic groups at the micellar surface. The terms b and c stop further micellar growth. A combination of eqs 1 and 10 with $V_1 = 69.45$ and $V_m = 9.21 \text{ cm}^3$ yields a calculated centroid volume $V_{c,\text{calcd}}$ for a given concentration.

On the other hand, Bottari and Festa proposed that all aggregates of TDC are multiples of the trimer:¹²

$$3A_1^{K_3} = A_3 \quad (11)$$

$$K_3 = [A_3]/C_1^3 \quad (12)$$

$$A_{3i-3} + A_3^{\beta_i} = A_{3i} \quad (i = 2, 3, 4, \dots, \infty) \quad (13)$$

$$\beta_i = [A_{3i}]/[A_{3i-3}][A_3] \quad (14)$$

$$C = C_1 + 3K_3C_1^3 + 6K_3^2\beta_2C_1^6 + 9K_3^3\beta_2\beta_3C_1^9 + 3K_3^4\beta_2\beta_3\beta_4C_1^{12} + (4 - 3K_3\beta_3C_1^3)/(1 - K_3\beta_3C_1^3)^2 \quad (15)$$

Here K_3 denotes the overall trimerization constant and β_i is a stepwise aggregation constant of trimer. By fitting of this model to the observed V_c values ($n = 19$), we determined best fit aggregation constants of $K_3 = 0.0102 \text{ M}^{-2}$, $\beta_2 = 5.566 \text{ M}^{-1}$, $\beta_3 = 14.993 \text{ M}^{-1}$, $\beta_4 = 14.000 \text{ M}^{-1}$, and $\beta_5 = \beta_6 = \dots = \beta = 15.464 \text{ M}^{-1}$. Further increases in adjustable parameters did not improve the SS value. The SS value for the Bottari–Festa model is 2.322 cm^6 , and it is worse than 0.348 cm^6 for our IV-8 model.

Furthermore, we simulated the derivative chromatograms at $C = 1.500$ and 2.003 mM on the basis of the two aggregation models for TDC. These concentrations are close to a cmc of 1.6 mM .⁴ As Figure 3 shows, our model is slightly better fit to the observed chromatogram at $C = 1.500$ mM than the Bottari–Festa model. The derivative chromatogram simulated on the basis of the Bottari–Festa model has an expansion in the region of lower elution volumes. This expansion is ascribed to an overestimation of trimer and the neglect of dimer. The simulated derivative chromatogram by the Bottari–Festa model at $C =$

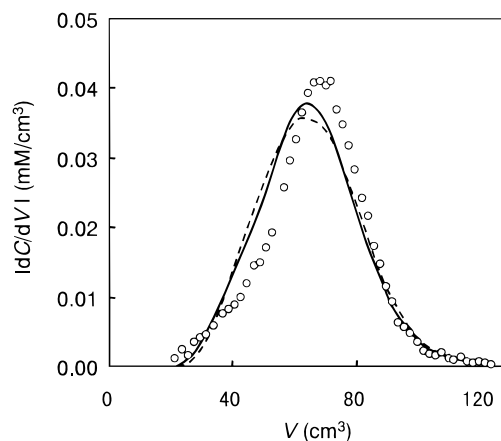


Figure 3. Derivative chromatograms of TC at $C = 1.500$ mM: (○) observed results; (—) simulation on the basis of our IV-8 model; (---) simulation on the basis of the Bottari–Festa model.

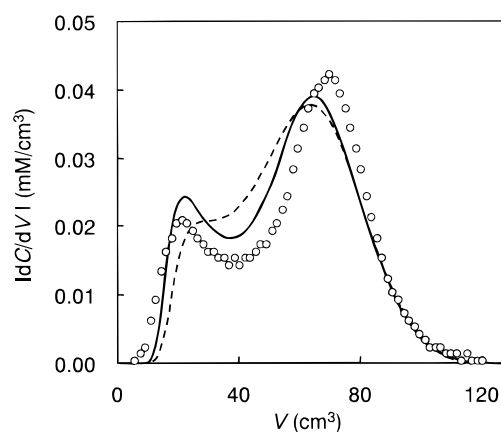


Figure 4. Derivative chromatograms of TC at $C = 2.003$ mM: (○) observed results; (—) simulation on the basis of our IV-8 model; (---) simulation on the basis of the Bottari–Festa model.

2.003 mM has a much shallower valley than the observed one, whereas that simulated by our model well reproduces a deep valley.

Thus, our IV-8 model is better than the Bottari–Festa model.

In crystals, TDC forms helices composed of multiples of trimer.¹⁸ The trimer is stabilized by polar interactions among three headgroups, and the three hydrophobic groups form the outer surface of the trimer. It is suggested that this structure of trimer, a reverse micelle, exists in water.¹⁸ This reverse micelle is expected to be more stable in organic solvent, but actually bile salts do not self-associate in methanol or ethanol.^{19,20} H NMR data suggested that bile salts form micelles by hydrophobic interactions.^{19,21} Barnes found that each of sodium cholate and rubidium deoxycholate forms dimer by hydrophobic interactions in crystals.²² Li and McGown proposed hydrophobic association models for the micelles of bile salts optimized by molecular mechanical calculations.⁹

The degree, β_c , of counterion binding is a matter of controversy in relation to the structure of bile salt micelles. Measurements of pNa²³ and self-diffusion coefficients²⁴ yielded values of $\beta_c = 0.03$ – 0.16 and $\beta_c = 0.1$ – 0.2 for sodium cholate. Using a taurocholate selective electrode, Ryu et al. showed that sodium taurocholate forms small micelles with little counterion binding.²⁵ The molar conductance versus concentration curve for sodium glycodeoxycholate exhibits a large hump around a cmc.²⁶ This hump indicates the presence of small micelles with little counterion binding. On the other hand, Bottari and Festa estimated the degree of counterion binding in taurodeoxycholate

solutions containing sodium ion, tetramethylammonium ion, barium ion, hydrogen ion, and the solid of sodium taurodeoxycholate by electromotive force measurements. They suggested that the total degrees of binding of sodium ion and hydrogen ion were 0.8 or more, irrespective of complete neglect of binding of tetramethylammonium ion and barium ion. Furthermore, they considered that the trimer of sodium taurocholate is in completely neutral form.¹² Their results are highly unlikely, compared to voluminous data on aqueous micelles. Briganti et al. reported that the degree of sodium ion binding to taurocholate micelles in tetramethylammonium chloride solutions ranged from 0.55 to 0.82 and changed abruptly around 0.35 M of tetramethylammonium chloride.¹⁸ Their β_c values seem to be too large, irrespective of the complete neglect of tetramethylammonium ion binding. Furthermore, it will be difficult to explain such an abrupt change in sodium ion binding.

In conclusion, our stepwise models for the self-association of TC and TDC are more rigorous than others. Their dimers exist together with higher multimers. TC and TDC form polydisperse micelles.

Acknowledgment. Thanks are due to Ms. Tomoko Okuda and Mr. Ryo Imaizumi for calculations.

References and Notes

- (1) Small, D. M. In *Chemistry*; Nair, P. P., Kritchevsky, D., Eds.; The Bile Acids; Plenum Press: New York, 1971; Vol. 1, Chapter 8.
- (2) Carey, M. C. In *Sterols and Bile Acids*; Danielsson, H., Sjovall, J., Eds.; Elsevier: Amsterdam, The Netherlands, 1985; Chapter 8.
- (3) Kratochvil, J. P. *Adv. Colloid Interface Sci.* **1986**, *26*, 131.
- (4) Funasaki, N.; Ueshiba, R.; Hada, S.; Neya, S. *J. Phys. Chem.* **1994**, *98*, 11541 and references therein.
- (5) Funasaki, N.; Hada, S.; Neya, S. *Bull. Chem. Soc. Jpn.* **1994**, *65*, 65.
- (6) Funasaki, N. *Adv. Colloid Interface Sci.* **1993**, *43*, 87. Funasaki, N.; Hada, S.; Neya, S. *Trends Phys. Chem.* **1997**, *6*, 253.
- (7) Funasaki, N. In *Bile Acid/Salt Surfactant Systems*; Hinze, W. L., Ed.; Organized Assemblies in Chemical Analysis; Jai Press: Greenwich; Vol. 2, in press.
- (8) Li, G.; McGown, L. B. *J. Phys. Chem.* **1993**, *97*, 6745.
- (9) Li, G.; McGown, L. B. *J. Phys. Chem.* **1994**, *98*, 13711.
- (10) Coello, A.; Meijide, F.; Nunez, E. R.; Tato, J. V. *J. Pharm. Sci.* **1996**, *85*, 9.
- (11) Liu, C. L. *J. Phys. Chem.* **1997**, *101*, 7055.
- (12) Bottari, E.; Festa, M. R. *Langmuir* **1996**, *12*, 1777.
- (13) Kratochvil, J. P.; Hsu, W. P.; Jacobs, M. A.; Aminabhavi, T. M.; Mukunoki, Y. *Colloid Polym. Sci.* **1983**, *261*, 781.
- (14) Ackers, G. K.; Thompson, T. E. *Proc. Natl. Acad. Sci. U.S.A.* **1965**, *53*, 342.
- (15) Lee, P. H.; Higuchi, W. I.; Daabis, N. A.; Noro, S. *J. Pharm. Sci.* **1985**, *74*, 880.
- (16) Ammon, H. V.; Walter, L. G. *Anal. Chem.* **1982**, *54*, 2079.
- (17) Mukerjee, P. *J. Phys. Chem.* **1972**, *76*, 565.
- (18) Briganti, G.; D'Archivio, A. A.; Galantini, L.; Giglio, E. *Langmuir* **1996**, *12*, 1180.
- (19) Small, D. M.; Penkett, S. A.; Chapman, D. *Biochim. Biophys. Acta* **1969**, *176*, 178.
- (20) Campredon, M.; Quiroa, V.; Thevand, A.; Iiouche, A.; Pouzard, G. *Magn. Reson. Chem.* **1986**, *24*, 624.
- (21) Stevens, R. D.; Ribeiro, A. A.; Lack, L.; Killenberg, P. G. *J. Lipid Res.* **1992**, *33*, 21.
- (22) Barnes, S. *Hepatology* **1984**, *4*, 98S.
- (23) Coello, A.; Meijide, F.; Nunez, E. R.; Tato, V. *J. Phys. Chem.* **1993**, *97*, 10186.
- (24) Lindman, B.; Kamenka, N.; Brun, B. *J. Colloid Interface Sci.* **1976**, *56*, 328.
- (25) Ryu, K.; Lowery, J. M.; Evans, D. F.; Cussler, E. L. *J. Phys. Chem.* **1983**, *87*, 5015.
- (26) Sesta, B.; D'Aprano, A.; Princi, A.; Filippi, C.; Iammarino, M. *J. Phys. Chem.* **1992**, *96*, 9545.